

Josephson tunnel junction controlled by quasiparticle injection

Francesco Giazotto*

NEST-INFM and Scuola Normale Superiore, I-56126 Pisa, Italy

Jukka P. Pekola

Low Temperature Laboratory, Helsinki University of Technology, P.O. Box 3500, FIN-02015 HUT, Finland

A Josephson tunnel junction transistor based on quasiparticle injection is proposed. Its operation relies on the manipulation of the electron distribution in one of the junction electrodes. This is accomplished by injecting quasiparticle current through the junction electrode by two additional tunnel coupled superconductors. Both large supercurrent enhancement and fast quenching can be achieved with respect to equilibrium by varying quasiparticle injection for proper temperature regimes and suitable superconductor combinations. Joined with large power gain this makes the device attractive for applications where reduced noise and low power dissipation are required.

PACS numbers: 73.20.-r, 73.23.-b, 73.40.-c

The control of Josephson currents as for the realization of efficient transistors has gained recently a rekindled interest [1]. A novel development in mesoscopic superconductivity is indeed represented by controllable superconductor(S)-normal metal(N)-superconductor(S) metallic weak links [2], where supercurrent suppression is achieved by altering the quasiparticle distribution in the N region through current injection. So far there have been a few successful demonstrations of this operation principle [3]. On the other hand, as recently proposed [4] and experimentally demonstrated [5], a SINIS control line (where I is a tunnel barrier) is particularly suitable for tuning Josephson current, allowing both enhancement and suppression with respect to equilibrium. Operation of these devices is based on the modification of the quasiparticle distribution in the N region of the junction. In this letter, we propose an *all*-superconducting tunnel junction device in which transistor effect is obtained by driving the electron distribution out of equilibrium in the superconductor. This is performed by voltage biasing a SISIS line (see Fig. 1) where the interelectrode is one of the two terminals belonging to the Josephson junction.

As compared to the hybrid devices above the present one benefits from the sharp characteristics due to the presence of superconductors with unequal energy gaps. We consider different superconductors S_1 and S_2 with energy gaps Δ_1 and Δ_2 (and critical temperatures $T_{c1,2}$), respectively, and we assume $\Delta_2 < \Delta_1$ [6, 7]. Under voltage bias V_C across the $S_1IS_2IS_1$ line (see the inset of Fig. 1) the heat current from S_2 to S_1 is given by

$$\mathcal{P} = \frac{2}{e^2 R_T} \int_{-\infty}^{\infty} d\varepsilon \varepsilon \mathcal{N}_1(\varepsilon) \mathcal{N}_2(\varepsilon) [f_0(\varepsilon, T_{e2}) - f_0(\varepsilon, T_{e1})], \quad (1)$$

where $\tilde{\varepsilon} = \varepsilon - eV_C/2$, $f_0(\varepsilon, T)$ is the Fermi-Dirac distribution function, T_{ek} is the electron temperature in S_k , R_T is the normal-state resistance of each S_1IS_2 junction and

$\mathcal{N}_k(\varepsilon) = |\text{Re}[(\varepsilon + i\Gamma_k)/\sqrt{(\varepsilon + i\Gamma_k)^2 - \Delta_k^2}]|$ is the smeared [8] BCS density of states of S_k . Figure 1 shows the calculated [9] heat current versus bias voltage V_C at constant bath temperature $T_{bath} = T_{e1} = T_{e2} = 0.4 T_{c1}$ and for different values of Δ_2 . \mathcal{P} is symmetric in V_C and it

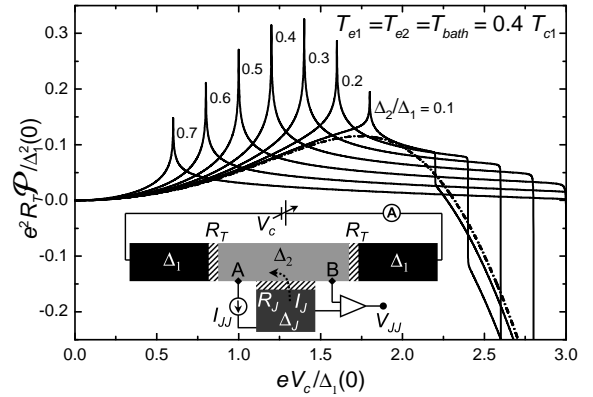


FIG. 1: Heat current \mathcal{P} out from S_2 by a $S_1IS_2IS_1$ line vs control voltage V_C at $T_{e1} = T_{e2} = T_{bath} = 0.4 T_{c1}$ for several Δ_2/Δ_1 ratios. Dash-dotted line represents \mathcal{P} when S_2 is in the normal state. Inset: Scheme of the Josephson device. The bias V_C across the $S_1IS_2IS_1$ line allows to control the supercurrent I_J (along the dashed line) increasing or suppressing its amplitude with respect to equilibrium. **A** and **B** represent tunnel contacts used to inject and measure the supercurrent.

is positive for $V_C < 2|\Delta_1(T) + \Delta_2(T)|/e$ thus allowing heat removal from S_2 , i.e., *hot* quasiparticle excitations are transferred to S_1 ; furthermore, the heat current is maximized at $V_C = \pm 2|\Delta_1(T) - \Delta_2(T)|/e$, where the finite-temperature logarithmic singularity occurs [6] (in a real situation it will be somewhat broadened by smearing in the density of states [6, 7, 8]). From Fig. 1 it follows that a positive heat current from S_2 exists only if $\Delta_2(T) < \Delta_1(T)$ holds. The dash-dotted line represents the heat current in the system when S_2 is in the normal state. Notably, when S_2 is in the superconducting state \mathcal{P} can largely exceed that one in the normal state.

*Electronic address: giazotto@sns.it

Then, on approaching $V_C = \pm 2|\Delta_1(T) + \Delta_2(T)|/e$, a sharp transition brings \mathcal{P} to negative values. An additional superconducting electrode S_J is connected to S_2 through a tunnel barrier so to realize a S_JIS_2 Josephson junction. S_J is characterized by its own energy gap Δ_J (different in general from $\Delta_{1,2}$) with critical temperature T_{cJ} , and R_J is the normal-state resistance of the junction. As we shall prove this transistor operation relies on the quasiparticle distribution established in S_2 upon voltage biasing the control line.

We consider a transport regime where strong inelastic electron-electron interaction forces the system to retain a local thermal (*quasi*)equilibrium, so that the quasiparticle distribution in S_2 is described by a Fermi function at temperature T_{e2} differing in general from T_{bath} . In order to determine the actual T_{e2} upon biasing with V_C we need to include those scattering mechanisms that transfer energy in S_2 . At the typical operation temperatures the predominant contribution comes from electron-phonon scattering that transfers energy between electrons and phonons. This heat flux is given by $\mathcal{P}_{e2-bath} = \Sigma \mathcal{V}(T_{e2}^5 - T_{bath}^5)$ [10], where Σ is a material-dependent parameter and \mathcal{V} is the volume of S_2 . The temperature T_{e2} is then determined by solving the energy-balance equation $\mathcal{P}(V_C, T_{bath}, T_{e2}) + \mathcal{P}_{e2-bath} = 0$.

The supercurrent (I_J) flowing through the S_JIS_2 junction can be calculated from [1, 11]:

$$I_J = -\frac{\sin \phi}{2eR_J} \int_{-\infty}^{\infty} d\varepsilon \{ \mathbf{f}_2(\varepsilon) \text{Re} \mathcal{F}_2(\varepsilon) \text{Im} \mathcal{F}_J(\varepsilon) + \mathbf{f}_J(\varepsilon) \text{Re} \mathcal{F}_J(\varepsilon) \text{Im} \mathcal{F}_2(\varepsilon) \}, \quad (2)$$

where ϕ is the phase difference between the superconductors, $\mathbf{f}_{2,J}(\varepsilon) = \tanh[\varepsilon/2k_B T_{e2,bath}]$ and $\mathcal{F}_{2,J}(\varepsilon) = \Delta_{2,J}/\sqrt{(\varepsilon + i\Gamma_{2,J})^2 - \Delta_{2,J}^2}$. In the aforementioned expressions we set $\Delta_2 = \Delta_2(T_{e2})$ and $\Delta_J = \Delta_J(T_{bath})$. Equation (2) shows that, for fixed T_{bath} and phase difference, the Josephson current is controlled by T_{e2} . The solution of the balance equation for T_{e2} combined with Eq. (2) yields the dimensionless transistor output characteristic shown in Fig. 2(a) [12], where I_J is plotted versus V_C at different bath temperatures, for $T_{c2} = 0.3 T_{c1}$ and $T_{cJ} = T_{c1}$. For $T_{bath} < T_{c2}$, I_J first increases monotonically up to $eV_C = 2[\Delta_1(T_{bath}) - \Delta_2(T_{e2})]$, where the cooling power is maximized; then it starts to slightly decrease after which it is rapidly quenched at $eV_C = 2[\Delta_1(T_{bath}) + \Delta_2(T_{e2})]$. Notably, even at bath temperatures exceeding T_{c2} (i.e., for $T_{bath} \geq T_{c2}$ where I_J is zero at equilibrium), a finite supercurrent is obtained at a voltage for which S_2 is brought into the superconducting state, after which I_J is recovered up to a large extent. The influence of different S_J on the supercurrent is displayed in Fig. 2(b) that shows I_J versus V_C at $T_{bath} = 0.8 T_{c2}$ for different T_{cJ}/T_{c1} ratios. As a consequence I_J is enhanced upon increasing Δ_J , being nearly doubled for $T_{cJ}/T_{c1} = 10$.

Figure 3(a) displays the transistor power dissipation $P = V_C I_C$, where I_C is the control current in the

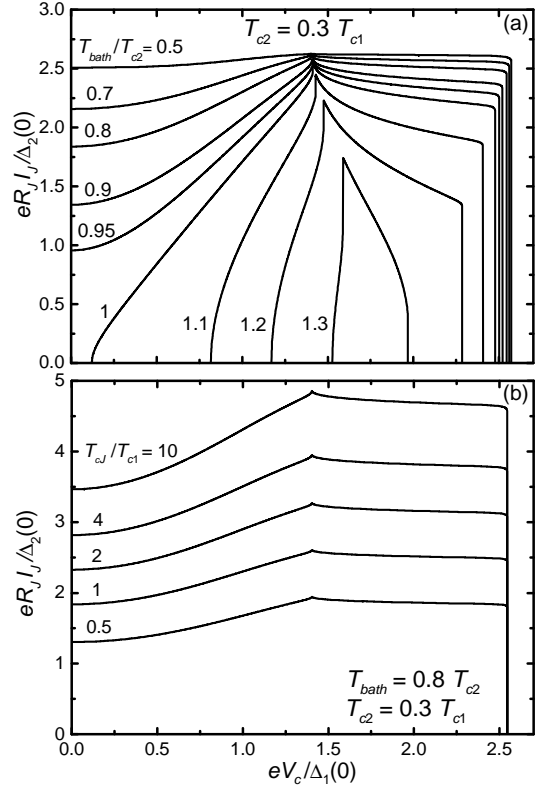


FIG. 2: (a) Supercurrent I_J vs control voltage V_C calculated at different bath temperatures T_{bath} for $T_{c2} = 0.3 T_{c1}$ (corresponding roughly to the Ti/Al combination) and $T_{cJ} = T_{c1}$. Note the sharp I_J suppression at $eV_C = 2[\Delta_1(T_{bath}) + \Delta_2(T_{e2})]$. (b) Supercurrent vs V_C calculated for several T_{cJ}/T_{c1} ratios at $T_{bath} = 0.8 T_{c2}$ and for $T_{c2} = 0.3 T_{c1}$.

$S_1IS_2IS_1$ line, calculated for $T_{c2} = 0.3 T_{c1}$ and $T_{cJ} = T_{c1}$ at different bath temperatures. The plot shows that at the lowest temperatures P obtains values of the order of some fW in the regime of supercurrent enhancement while of some hundred of fW around the I_J quenching. This is because of low control currents through the structure. As far as noise is concerned, the total input noise per unit bandwidth $\langle \delta I_{tot}^2 \rangle$ [13] in the control line can be expressed as [14]

$$\langle \delta I_{tot}^2 \rangle = \langle \delta I_C^2 \rangle - 2S_{IC} \langle \delta \mathcal{P} \delta I_C \rangle + S_{IC}^2 \langle \delta \mathcal{P}^2 \rangle, \quad (3)$$

where

$$\langle \delta I_C^2 \rangle = \frac{1}{R_T} \int_{-\infty}^{\infty} d\varepsilon \mathcal{N}_1(\varepsilon) \mathcal{N}_2(\varepsilon) \mathcal{W}(\varepsilon, \varepsilon), \quad (4)$$

$$\langle \delta \mathcal{P}^2 \rangle = \frac{1}{e^2 R_T} \int_{-\infty}^{\infty} d\varepsilon \varepsilon^2 \mathcal{N}_1(\varepsilon) \mathcal{N}_2(\varepsilon) \mathcal{W}(\varepsilon, \varepsilon), \quad (5)$$

$$\langle \delta \mathcal{P} \delta I_C \rangle = -\frac{1}{e R_T} \int_{-\infty}^{\infty} d\varepsilon \varepsilon \mathcal{N}_1(\varepsilon) \mathcal{N}_2(\varepsilon) \mathcal{W}(\varepsilon, \varepsilon), \quad (6)$$

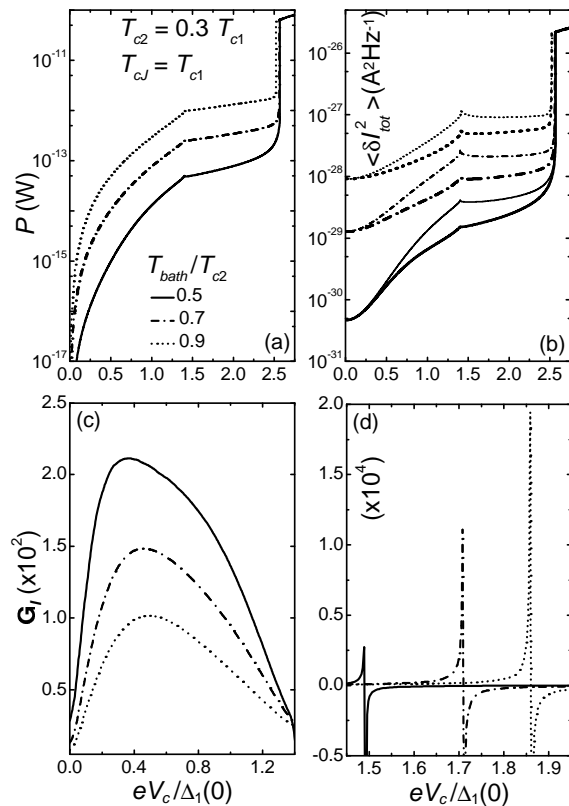


FIG. 3: (a) Dissipated power P and (b) total input noise $\langle \delta I_{tot}^2 \rangle$ in the $S_1IS_2IS_1$ line against V_C . The transistor current gain $G_I(V_C)$ is shown in (c) and (d) in two different ranges of V_C . All these calculations are performed for $T_{c2} = 0.3 T_{c1}$, $T_{cJ} = T_{c1}$ and at three different bath temperatures.

and $\mathcal{W}(\varepsilon, \tilde{\varepsilon}) = f_0(\varepsilon, T_{e2})(1 - f_0(\tilde{\varepsilon}, T_{bath})) + f_0(\tilde{\varepsilon}, T_{bath})(1 - f_0(\varepsilon, T_{e2}))$. Equations (4), (5) and (6) represent fluctuations due to charge and heat flow, and their mutual correlation, respectively, and S_{IC} is the zero-frequency current responsivity, $S_{IC}(V_C) = (\partial I_C / \partial T_{e2}) / (5 \Sigma V T_{e2}^4 + \partial \mathcal{P} / \partial T_{e2})$ [14]. $\langle \delta I_{tot}^2 \rangle$ is displayed in Fig. 3(b) for the same parameters as in Fig. 3(a), and shows that input noise as low as some $10^{-30} \text{ A}^2 \text{ Hz}^{-1}$ can be achieved in

the enhancement regime while of some $10^{-29} \text{ A}^2 \text{ Hz}^{-1}$ at the quenching voltage. Thin lines are the *uncorrelated* noise power, i.e., the noise obtained by adding the contributions of Eqs. (4) and (5) only. Notably, the impact of mutual correlations (Eq. (6)) is easily recognized leading to significant noise reduction ($\sim 50\%$) in the range of supercurrent enhancement.

We shall further comment on the available gain. Input ($V_{in} = V_C \sim \Delta_1$) and output ($V_{out} = I_J R_J \sim \Delta_2$) (see also Fig. 2(b)) voltages allow a voltage gain $G_V = V_{out}/V_{in} \sim \Delta_2/\Delta_1$ so that with realistic parameters G_V is not much smaller than 1. The differential current gain, defined as $G_I = dI_J/dI_C = (\frac{dI_J}{dV_C})(\frac{dI_C}{dV_C})^{-1}$, is plotted in Fig. 3(c,d) in two different bias ranges for some values of T_{bath} . The figure shows that G_I obtains large values with some 10^2 in the regime of supercurrent enhancement and several 10^3 below the quenching. The corresponding input impedance ranges from hundreds of k Ω to tens of M Ω , respectively. In order to exploit the power gain (G_P) the Josephson junction needs to be operated in the dissipative regime; in such a situation an estimate for the achievable power gain [4] yields $G_P \sim 10^2 \dots 10^3$ depending on the operating V_C and bias current I_{JJ} across the junction (see Fig. 1). One should note that such a large power gain, not achievable, e.g., using a SINIS controlled SNS transistor [4] in the same transport regime, is an additional advantage of the present scheme.

We conclude with some further benefits of our proposal. Due to the presence of the superconducting inter-electrode, highly transmissive tunnel junctions are not necessary unlike in SINIS devices. The device is also less sensitive to thermal fluctuations as compared to SNS junctions [5]. Furthermore, it is easier to fabricate taking advantage of the well established metal-based tunnel junction technology. A promising choice for transistor and switch implementations could be a combination of Al and Ti.

The authors acknowledge the Large Scale Installation Program ULTI-3 of the European Union and the Academy of Finland (TULE program) for financial support, and D. Golubev, T. T. Heikkilä, A. M. Savin and H. Seppä for fruitful discussions.

-
- [1] See, for example, A.A. Golubov, M.Yu. Kupriyanov, and E. Il'ichev, Rev. Mod. Phys. **76**, 411 (2004).
 - [2] F.K. Wilhelm, G. Schön, and A.D. Zaikin, Phys. Rev. Lett. **81**, 1682 (1998).
 - [3] J.J.A. Baselmans, A.F. Morpurgo, B.J. van Wees, and T.M. Klapwijk, Nature (London) **397**, 43 (1999); J. Huang, F. Pierre, T.T. Heikkilä, F.K. Wilhelm, and N.O. Birge, Phys. Rev. B **66**, 020507 (2002); R. Shaikhaidarov, A.F. Volkov, H. Takayanagi, V.T. Petrashov, and P. Delsing, Phys. Rev. B **62**, R14649 (2000).
 - [4] F. Giazotto, T.T. Heikkilä, F. Taddei, R. Fazio, J.P. Pekola, and F. Beltram, Phys. Rev. Lett. **92**, 137001 (2004); F. Giazotto, F. Taddei, T.T. Heikkilä, R. Fazio, and F. Beltram, Appl. Phys. Lett. **83**, 2877 (2003).
 - [5] A.M. Savin, J.P. Pekola, J.T. Flyktman, A. Anthore, and F. Giazotto, Appl. Phys. Lett. **84**, 4179 (2004).
 - [6] B. Frank and W. Krech, Phys. Lett. A **235**, 281 (1997).
 - [7] A.J. Manninen, J.K. Suoknuuti, M.M. Leivo, and J.P. Pekola, Appl. Phys. Lett. **74**, 3020 (1999).
 - [8] J.P. Pekola, T.T. Heikkilä, A.M. Savin, J.T. Flyktman, F. Giazotto, and F.W.J. Hekking, Phys. Rev. Lett. **92**, 056804 (2004).
 - [9] We assume throughout the paper a realistic smearing parameter $\Gamma_k = 10^{-4} \Delta_k$ (see Ref. [8]).
 - [10] F.C. Wellstood, C. Urbina, and J. Clarke, Phys. Rev. B **49**, 5942 (1994).

- [11] T.T. Heikkilä, private communication.
- [12] For the calculation we choose $\phi = \pi/2$, $T_{c1} = 1.19$ K (Al), $R_T = 10^3 \Omega$, $R_J = 300 \Omega$, $\mathcal{V} = 0.1 \mu\text{m}^3$ and $\Sigma = 10^{-9} \text{WK}^{-5} \mu\text{m}^{-3}$ (Ti) (see Ref. [7]).
- [13] We suppose each junction to contribute in an uncorrelated way to the total noise.
- [14] D. Golubev and L. Kuzmin, J. Appl. Phys. **89**, 6464 (2001).